

Pulsed coherent population trapping with repeated queries for producing single-peaked high contrast Ramsey interference

Z. Warren, M. S. Shahriar, R. Tripathi, and G. S. Pati

Citation: *Journal of Applied Physics* **123**, 053101 (2018); doi: 10.1063/1.5008402

View online: <https://doi.org/10.1063/1.5008402>

View Table of Contents: <http://aip.scitation.org/toc/jap/123/5>

Published by the *American Institute of Physics*

Articles you may be interested in

[One-dimensional dielectric bi-periodic photonic structures based on ternary photonic crystals](#)

Journal of Applied Physics **123**, 043101 (2018); 10.1063/1.5011637

[Optical properties of electrically connected plasmonic nanoantenna dimer arrays](#)

Journal of Applied Physics **123**, 063101 (2018); 10.1063/1.5008511

[Guest Editorial: The dawn of gallium oxide microelectronics](#)

Applied Physics Letters **112**, 060401 (2018); 10.1063/1.5017845

[Observation of Goos-Hänchen shift in plasmon-induced transparency](#)

Applied Physics Letters **112**, 051101 (2018); 10.1063/1.5016481

[Intrinsic terahertz photoluminescence from semiconductors](#)

Applied Physics Letters **112**, 041101 (2018); 10.1063/1.5012836

[Experimental research on time-resolved evolution of cathode plasma expansion velocity in a long pulsed magnetically insulated coaxial diode](#)

Journal of Applied Physics **123**, 073301 (2018); 10.1063/1.5017465

AIP | Journal of Applied Physics

SPECIAL TOPICS



Pulsed coherent population trapping with repeated queries for producing single-peaked high contrast Ramsey interference

Z. Warren,¹ M. S. Shahriar,^{2,3} R. Tripathi,¹ and G. S. Pati^{1,a)}

¹*Department of Physics and Engineering, Delaware State University, Dover, Delaware 19901, USA*

²*Department of Electrical Engineering and Computer Science, Northwestern University, Evanston, Illinois 60308, USA*

³*Department of Physics and Astronomy, Northwestern University, Evanston, Illinois 60308, USA*

(Received 5 October 2017; accepted 19 January 2018; published online 6 February 2018)

A repeated query technique has been demonstrated as a new interrogation method in pulsed coherent population trapping for producing single-peaked Ramsey interference with high contrast. This technique enhances the contrast of the central Ramsey fringe by nearly 1.5 times and significantly suppresses the side fringes by using more query pulses (>10) in the pulse cycle. Theoretical models have been developed to simulate Ramsey interference and analyze the characteristics of the Ramsey spectrum produced by the repeated query technique. Experiments have also been carried out employing a repeated query technique in a prototype rubidium clock to study its frequency stability performance. *Published by AIP Publishing.* <https://doi.org/10.1063/1.5008402>

I. INTRODUCTION

For attaining high precision, atomic clock technologies rely on using atomic resonances with narrow linewidth and a high signal-to-noise ratio (*SNR*). In this context, coherent population trapping (CPT) has been widely investigated for realizing compact (chip-scale) atomic clocks and magnetometers with high precision.^{1–6} CPT is produced by continuous Raman excitation in a three-level Λ -system formed by two metastable ground-states coupled to a common excited state in alkali atoms, and it is capable of producing a narrow-linewidth “dark state” resonance.^{7–9} The linewidth of CPT resonance is fundamentally determined by the inverse of the ground-state coherence lifetime which could be many milliseconds long in a vapor medium.¹⁰ However, in practice, the linewidth is broadened due to the higher optical power used in experiments to achieve high contrast (or *SNR*) in CPT resonance.^{11,12} To overcome power-broadening and achieve high contrast, an alternative pulsed CPT scheme has been explored.^{13–22} Instead of continuous excitation, pulsed excitation is used with a pulse sequence comprising a long CPT (or preparation) pulse and a short query pulse. Ramsey interference is produced during read-out by the query pulse after an interaction free-evolution of the “dark state” for time T . The fringe-width $\Delta\nu = 1/2T$ associated with Ramsey interference is independent of the optical power used. Therefore, a narrow fringe-width can be produced by choosing a large T ; however, the maximum T is limited by the dephasing time of the medium. A notable advantage of the pulsed CPT scheme is that strong interaction of atoms with resonant light has been shown to reduce the light shift,^{23,24} thereby enhancing long-term frequency stability. In a practical situation, however this advantage could be lost due to off-resonant light shifts produced by sideband frequencies^{25,26} or incoherent light pedestals.²⁷ The Ramsey technique has also been used to measure ground-state relaxation times in atomic

vapors for atomic clock and quantum information processing applications.^{28–30}

Typically, in pulsed CPT, multiple Ramsey fringes are generated as the frequency difference between the laser fields is varied around the two-photon resonance condition.^{13,16} The central fringe is used for realizing the Ramsey clock. However, the central fringe is often indistinguishable from the side fringes, since the amplitudes of the side fringes are nearly equal to that of the central fringe. This can potentially create difficulties in the Ramsey clock while engaging its electronic servo to lock (or relock) to the peak of the central fringe. Guérandel *et al.* developed a phase-stepping mechanism¹⁵ and later, Yun *et al.* extended this to a multi-pulse phase-stepping scheme³¹ for producing high-contrast in the central Ramsey fringe. In these schemes, due to the phase shift, the central Ramsey fringe assumes a dispersive line-shape, which is convenient for use as a control signal in the Ramsey clock. However, the disadvantage is that phase-stepping process requires precise adjustment of the relative-phase between the two laser frequencies, which can be difficult to implement. Any potential phase error introduced in this process can lead to a frequency error, thus limiting the clock stability. Performance of the multi-pulse phase-stepping scheme in the Ramsey clock has not been studied. On the other hand, high-contrast Ramsey fringes with contrast up to 50% have been reported by combining the push-pull optical pumping (PPOP)^{26,32,33} scheme with pulsed CPT. Magneto-optical rotation (MOR) has also been implemented in pulsed CPT for generating high-contrast Ramsey fringes having reduced (or zero) optical background.³⁴ Unlike multi-pulse phase-stepping, PPOP and MOR do not suppress the side fringes produced in Ramsey interference. However, implementation of PPOP escalates hardware complexity, and implementation of MOR requires $lin \parallel lin$ polarized CPT fields, which show high sensitivity to the magnetic field, which is detrimental to clock applications.^{35,36}

^{a)} Author to whom correspondence should be addressed: gspati@desu.edu

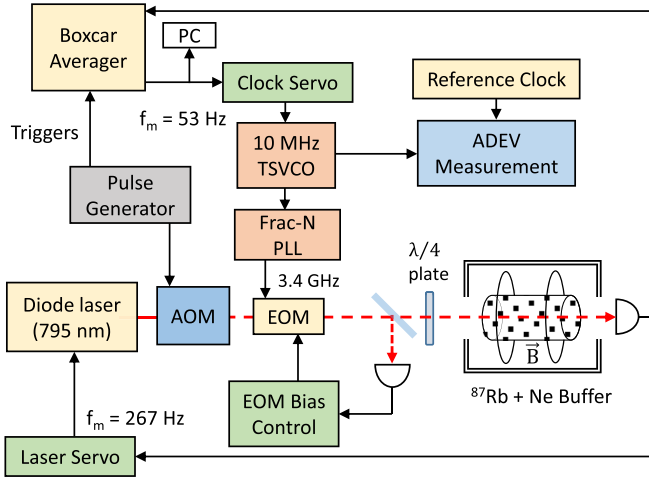


FIG. 1. Experimental setup used in implementing a rubidium Ramsey clock by employing SQT and RQT in the pulsed CPT scheme.

In this paper, we describe a repeated query technique (RQT) implemented in pulsed CPT for generating a single-peaked central Ramsey fringe with enhanced contrast and reduced side fringes. We have demonstrated that, compared to the single query technique (SQT) which has been commonly used in pulsed CPT, the RQT produces a central fringe with a higher contrast and a bigger SNR. Implementation of the RQT requires a simple modification of the pulse sequence, which has been achieved electronically, thus making RQT practically suitable for miniaturization of the Ramsey clock. We present experimental results as well as theoretical discussions to substantiate the advantages of RQT over SQT. Our theoretical discussions are based on two physical models: (a) atomic density-matrix model and (b) Fourier analysis of the pulse sequence. Experiments have been carried out to measure the frequency stability performance of a prototype Ramsey clock by implementing SQT and RQT in pulsed CPT. The rest of the paper is organized as follows: In Sec. II, we describe pulsed CPT experiments performed using SQT and RQT in a pure isotope rubidium cell. In Sec. III, we

present experimental results and theoretical discussions. At the end of this section, we discuss frequency stability performances of the prototype Ramsey clock.

II. EXPERIMENTAL DESCRIPTION

Figure 1 shows the diagram of our experimental setup used to study pulsed CPT with SQT and RQT. The setup was also used as a prototype Ramsey clock to study frequency stability performances with SQT and RQT. A frequency-modulated laser beam is created by sending light from a tunable single-frequency diode laser ($\lambda = 795$ nm, $\Delta\nu < 1$ MHz) through a fiber-coupled electro-optic modulator (EOM, bias $V_\pi = 1.4$ V). The EOM is driven by an RF signal with frequency close to half the hyperfine ground-state frequency (i.e., $\Delta\nu_{hf}/2 = 3.417$ GHz) of ^{87}Rb atoms. This creates optical sidebands with frequency-difference matching $\Delta\nu_{hf} = 6.834$ GHz. These optical sidebands further create a Λ -type Raman excitation [illustrated in Fig. 2(a)] and CPT phenomena in a small (2 cm long) rubidium cell. The EOM bias voltage is actively controlled to minimize the carrier optical power which is not used in the excitation process. This is achieved by measuring a small fraction of the beam after the EOM with a photodiode and using it as the “control signal” for holding the EOM bias voltage at the minimum carrier.³⁷ The RF signal driving the EOM is synthesized from a 10 MHz temperature-stabilized voltage controlled oscillator (TSVCO) with the help of a fractional-N phase-locked loop (frac-N PLL) electronic board.

Prior to the EOM, a free-space acousto-optic modulator (AOM, $f_c = 80$ MHz) is used as a switching element for generating pulse cycles, shown in Figs. 2(b) and 2(c), to conduct pulsed CPT experiments using SQT and RQT. For SQT, the pulse cycle [Fig. 2(b)] is defined by a CPT pulse of duration τ_c , free-evolution time T , and a single query pulse of duration τ_q . During our experiments, the cycle period τ_p is set to be 2.1 ms and τ_c is chosen to be $500 \mu\text{s}$ long for preparing the atoms in the dark state via optical pumping. The free-evolution time T is chosen to be 1.5 ms, based on the dephasing time of the

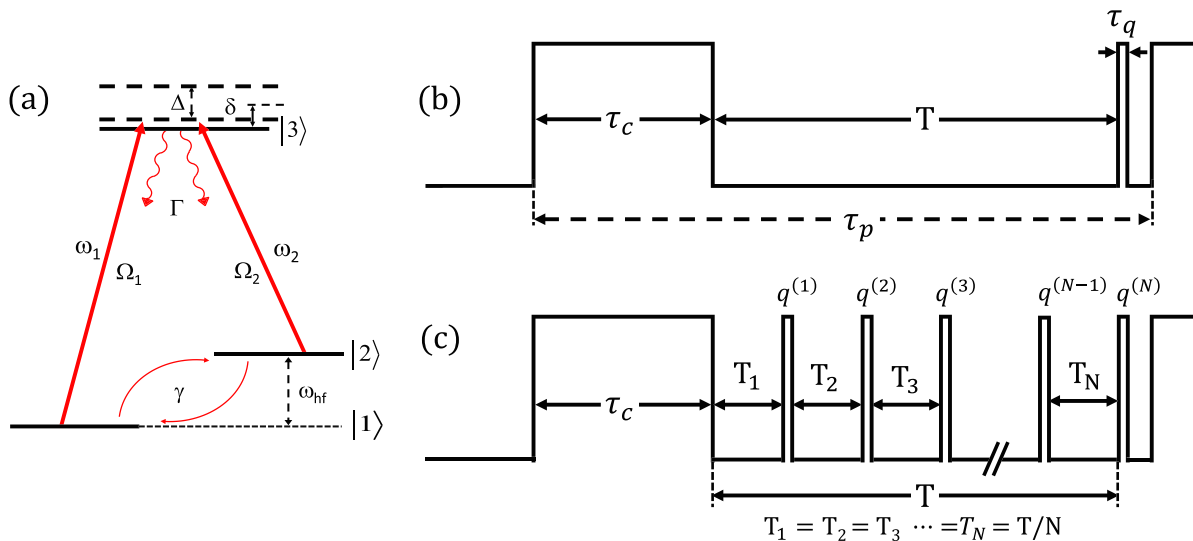


FIG. 2. (a) Diagram showing Raman excitation in a three-level Λ -type atomic system constructed in the D1 manifold of ^{87}Rb atoms. Timing diagrams showing pulse cycles for (b) SQT and (c) RQT used in the pulsed CPT scheme. Here, τ_p is the cycle period.

dark state in the rubidium cell used in our experiments. The duration of the query pulse τ_q is chosen to be short (i.e., 1 μ s) for minimizing its destructive read-out effect. Figure 2(c) shows the pulse cycle of RQT using a sequence of N repeated query pulses. In this case, the free-evolution time T corresponding to SQT is kept fixed and divided into N equal time periods (i.e., $T_1 = T_2 \dots = T_N = T/N$) as shown in the diagram. Therefore, a single pulse cycle of RQT consists of one CPT pulse of duration τ_c followed by a periodic train of N free-evolution times ($T_1, T_2 \dots T_N$) and N query pulses ($q^{(1)}, q^{(2)} \dots q^{(N)}$) each with duration τ_q .

The pulse generator driving the AOM is programmed to switch the AOM on or off at appropriate times depending on the implementation of SQT or RQT. The pulsed optical beam is passed through a quarter-wave ($\lambda/4$) plate to create circularly polarized CPT fields.³⁶ The experiment here could have been carried out using the double-Lambda scheme, employing the *lin||lin* configuration for the CPT fields. However, we chose to use the experimentally simpler approach of using two circularly polarized beams (TCPBs). Another reason for choosing this scheme is that, contrary to the *lin||lin* configuration, CPT under excitation with TCPBs is insensitive to the first-order Zeeman shift without requiring any delicate balance of the intensities, a property that is highly desirable for a practical clock. The optical beam is then passed through a pure isotope ⁸⁷Rb vapor cell (length = 2 cm, diameter = 1 cm) filled with 10 Torr neon buffer gas. It should be noted that CPT resonance excited by TCPBs has a surprisingly high contrast for the particular cell we used, even though it is in general not expected to prevent formation of trapped states. This was shown in a recent paper by us,³⁶ in which we studied CPT contrasts for various polarizations and transitions. Specifically, using TCPBs, we observed CPT contrast as high as $\sim 17\%$, using resonant excitation with the $F' = 2$ upper state. This contrast indicates that formation of trapped states was suppressed to some extent. The suppression of formation of trapped states could be due to a combination of reasons. These include pressure broadening of the atomic transitions and collision-induced population exchange.

The physics package of the vapor cell consists of a dual layer μ -metal magnetic-shield enclosure (attenuation $\simeq 40$ dB) and a pair of Helmholtz coils mounted inside the enclosure to apply a small uniform axial magnetic field ($B \simeq 100$ mG) for lifting Zeeman degeneracies of the magnetic sublevels. The vapor cell is also actively temperature controlled ($\Delta T \simeq 100$ mK). A boxcar averager is used for observing Ramsey interference by gating the photodetector output during the query pulse. Ramsey fringes are acquired by repeating pulse cycles and slowly changing the voltage to the TSVCO, thereby changing the frequency difference between the CPT fields around the ground-state hyperfine frequency (i.e., $\Delta\nu_{hf} = 6.834$ GHz) of ⁸⁷Rb atoms. While acquiring Ramsey fringes using RQT, the boxcar (SR250, Stanford Research Systems) was electronically triggered by N query pulse triggers, and the number of sample average in the boxcar was set equal to N . In the case of SQT, Ramsey fringes were measured using the integrated boxcar signal output corresponding to the lone transmitted query pulse. In the case of RQT, the signal from the boxcar is averaged over N

query pulses (or samples) using the internal averaging circuitry to produce Ramsey fringes. We also acquired Ramsey fringes directly using a computer interfaced digitizer board, and by implementing signal integration and averaging (similar to the boxcar) through NI LabVIEW. This provides the ability to perform real-time signal processing on the acquired Ramsey fringes.

During the experiments, the laser frequency is locked to the absorption maximum created by the optical sidebands by virtue of resonant excitations of the two sidebands with one of the hyperfine excited states in the ⁸⁷Rb D1 manifold.^{38,39} Thus, the output from a single photodetector (shown in Fig. 1) is used for executing the laser servo and the clock servo simultaneously. The two servos operated in tandem, but independently by dithering the laser frequency at two different modulation frequencies ($f_m = 267$ Hz and 53 Hz, respectively). Each individual servo consisted of an electronic module with a lock-in-amplifier and a proportional-integral (PI) controller, and the control signals for the servos were generated by demodulating the photodetector output at respective dither frequencies. This helped us in operating the experimental setup in Fig. 1 as a prototype Ramsey clock by simply engaging the clock servo. The stability of the locked TSVCO was then measured using a reference rubidium clock and the Allan deviation (ADEV) measuring instrument.

III. RESULTS AND DISCUSSION

Figures 3(a) and 3(b) show experimentally acquired Ramsey fringes using the SQT pulse cycle. We used $T = 1.5$ ms, $\tau_q = 1$ μ s, and a cycle period $\tau_p = 2.1$ ms. The duration of the CPT pulse, τ_c , was varied from 250 μ s to 500 μ s to show its effect on the fringe envelope. The fringes were acquired by keeping the average optical power in the CPT pulse at 24 μ W. This agreed with the continuous power (measured by keeping the switching AOM on) multiplied by the pulse duty cycle ($\simeq \tau_c/\tau_p$). When τ_c was increased to 500 μ s, the continuous power was lowered (by nearly a factor of 2) in order to maintain the average power at 24 μ W (or average intensity at 48 μ W/cm² for an approximate 8 mm beam diameter in the cell). This is done to prevent any change in fringe contrast and envelope induced due to the optical power. The voltage applied to the TSVCO was slowly scanned during the acquisition of the Ramsey fringes shown in Figs. 3(a) and 3(b). This produced a symmetric scanning of the laser frequencies ω_1 and ω_2 and hence, the difference frequency $\Delta = \frac{1}{2\pi}[(\omega_1 - \omega_2) - \omega_{hf}]$ around $\Delta = 0$. The fringe-widths in Figs. 3(a) and 3(b) were measured and found to match closely with $\Delta\nu_f (= 1/2T) \simeq 333$ Hz. We also measured the contrast, C of the central Ramsey fringe using the definition $C [= (V_P - V_B)/V_P]$, where $(V_P - V_B)$ is the amplitude of the central fringe, also considered as the “signal,” V_P is the peak, and V_B is the background, both measured in volts. The central Ramsey fringes in Figs. 3(a) and 3(b) have contrasts of approximately 47% and 59%, respectively. The contrast observed in the central fringe in Fig. 3(b) is higher due to higher Raman saturation effect (i.e., $\Omega\tau_c \simeq 25$).^{11,24} In both Figs. 3(a) and 3(b), the side fringes adjacent to the center have also been observed to possess high contrasts ($\simeq 41\%$

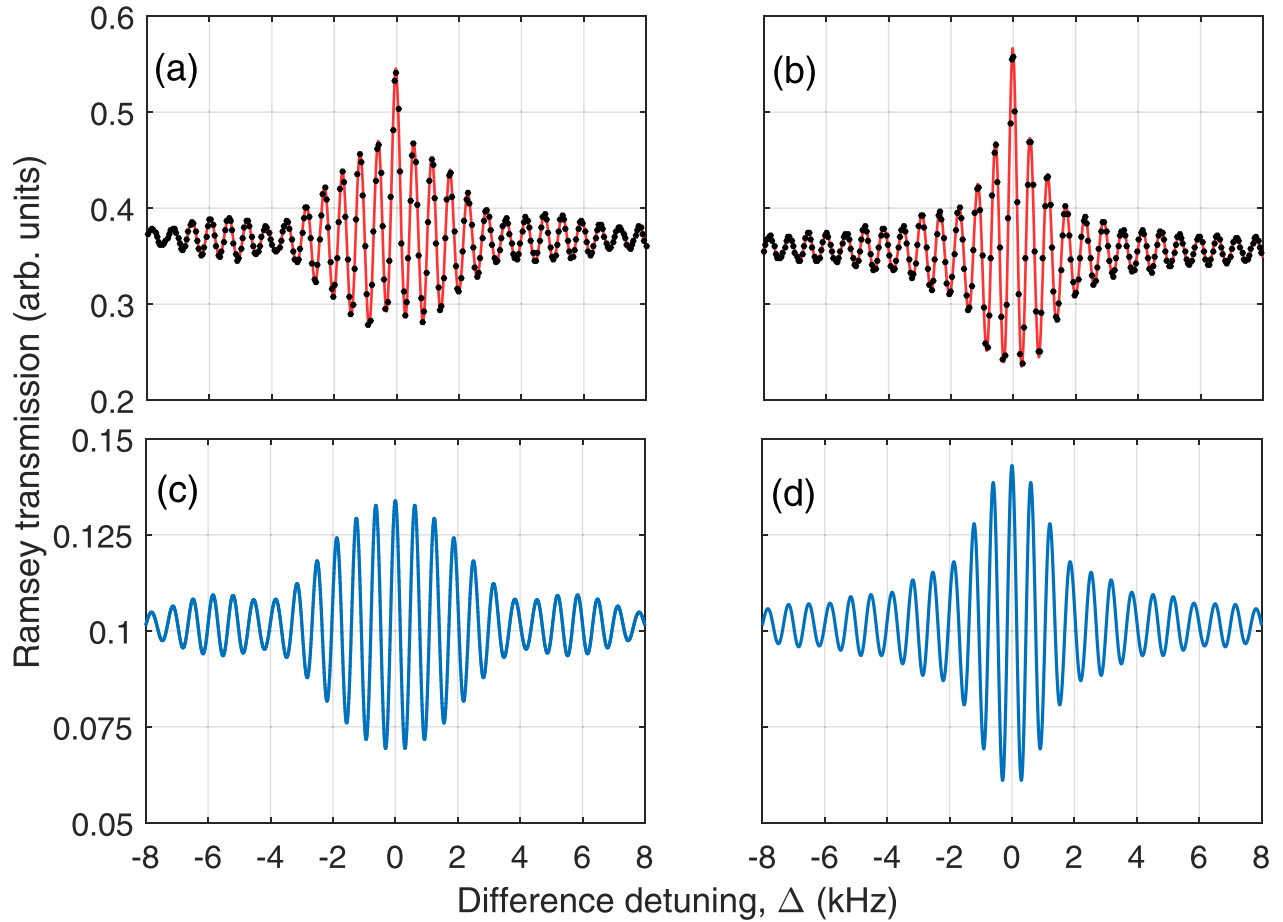


FIG. 3. Experimentally acquired Ramsey fringes using SQT ($N = 1$) for (a) $\tau_c = 250 \mu\text{s}$ and (b) $\tau_c = 500 \mu\text{s}$ and parameters: $T = 1.5 \text{ ms}$, $\tau_q = 1 \mu\text{s}$ and average optical power $24 \mu\text{W}$. Theoretically simulated Ramsey fringes using SQT for (c) $\tau_c = 250 \mu\text{s}$ and (d) $\tau_c = 500 \mu\text{s}$. The parameters used in simulations are $T = 1.5 \text{ ms}$, $\tau_q = 1 \mu\text{s}$, $\Omega = \Gamma/100$, $\Gamma = 6 \text{ MHz}$, $\delta = 0$, and $\gamma = 200 \text{ Hz}$.

and 50%, respectively), comparable to that of the central fringe. In the presence of these high-contrast side fringes, the central fringe cannot be readily distinguishable as an atomic reference to the electronic servo in the Ramsey clock.

We have theoretically investigated the above aspect of Ramsey interference by formulating pulsed CPT excitations in a three-level atomic system [Fig. 2(a)] using the density-matrix equations^{24,40} $\frac{\partial \rho}{\partial t} = -\frac{i}{\hbar} [H\rho - \rho H^\dagger] + L$, where ρ corresponds to the density operator represented by a (3×3) matrix, H is the semi-classical and non-Hermitian Hamiltonian that includes the effect of decays from atomic states, and L represents the source matrix accounting for influx of atoms decaying from one state to another. Applying rotating-wave approximation, the time-independent Hamiltonian H (setting $\hbar = 1$) used in our model is given by

$$\begin{pmatrix} \frac{\Delta}{2} - \frac{i\gamma}{2} & 0 & -\frac{\Omega_1}{2} \\ 0 & -\frac{\Delta}{2} - \frac{i\gamma}{2} & -\frac{\Omega_2}{2} \\ -\frac{\Omega_1}{2} & -\frac{\Omega_2}{2} & -\delta - \frac{i\Gamma}{2} \end{pmatrix}, \quad (1)$$

where Ω_1 and Ω_2 correspond to Rabi frequencies of the two coherent laser fields in Fig. 2(a), referred to as CPT fields, $\delta = (\delta_1 + \delta_2)/2$ corresponds to the average (or common-

mode) laser frequency detuning which is defined in terms of single-photon frequency detunings δ_1 and δ_2 of the two CPT fields, and $\Delta (= \delta_1 - \delta_2)$ corresponds to the difference frequency detuning of the CPT fields. For simplicity, our calculations assume equal Rabi frequencies (i.e., $\Omega_1 = \Omega_2 = \Omega$)

with $\Omega = \sqrt{\frac{\Omega_1^2 + \Omega_2^2}{2}}$ defined as the average Rabi frequency. The time-dependent density-matrix equations are solved numerically to calculate Ramsey interference produced by the SQT pulse cycle. Ramsey fringes are simulated by iterating numerical solutions for ρ after each SQT pulse cycle for different values of Δ around zero. We chose the imaginary component of density-matrix element ($\rho_{13} + \rho_{23}$) to simulate and study the characteristics of Ramsey fringes. Physically, $\text{Imag}(\rho_{13} + \rho_{23})$ is proportional to the absorption coefficient for the CPT fields.

Figures 3(c) and 3(d) show simulated Ramsey fringes using the SQT pulse cycle, using parameters similar to those used in the experiments. To draw comparisons with experiments, we chose $\Omega = \Gamma/100$ where $\Gamma = (2\pi)6 \times 10^6 \text{ s}^{-1}$ corresponds to the decay rate of the rubidium excited state, and introduced a ground-state relaxation rate $\gamma = (2\pi)2 \times 10^2 \text{ s}^{-1}$ in our model. Simulated Ramsey fringes in Figs. 3(c) and 3(d) show characteristics similar to those seen in Figs. 3(a) and 3(b) in terms of linewidths and fringe envelopes. The width of the envelope is attributable to a combination of

power-broadening and transit-time broadening, corresponding to the power in the CPT pulse and the duration (τ_c) thereof, respectively.

The contrasts of central Ramsey fringes in Figs. 3(c) and 3(d) are approximately 48% and 57%, respectively. Although these values of contrasts closely agree with the experimental results, the agreement is mostly a coincidence. Our model is based on an ideal three-level atomic system. In order to accurately estimate the fringe contrast, the model has to be extended to a multi-level atomic system^{36,40} and also needs to include various physical processes in a vapor cell such as velocity averaging, propagation of optical fields in the cell, and so on. Nevertheless, the ideal three-level model serves our purpose to investigate other characteristics of Ramsey fringes produced by using SQT and RQT in pulsed CPT.

Next, we extended the three-level model to calculate Ramsey fringes formed by RQT by simply including N query pulses in the pulse cycle. In this case, solutions to ρ were obtained for time interval τ_c first and then for time intervals (T/N and τ_q), repeated N times. The values of the relevant elements of ρ obtained after each query pulse $q^{(i)}$, $i = 1 \dots N$ are added to simulate Ramsey interference formed by RQT. Before presenting simulated results for RQT, we present our experimental results obtained using RQT by simply changing N electronically in the experiment.

Figures 4(a)–4(c) show Ramsey fringes produced by RQT for $N = 3, 5,$ and 10 , respectively. The parameters used for the RQT pulse cycles were $\tau_c = 500 \mu\text{s}$, $T = 1.5 \text{ ms}$, and $\tau_q = 1 \mu\text{s}$, with a pulse-sequence repetition interval of $\tau_p = 2.1 \text{ ms}$. The average optical power used in the CPT pulse was approximately $24 \mu\text{W}$. As can be seen, with increasing N , the central fringe becomes larger, and the side fringes close to the central one get suppressed. This suppression is due to interference among multiple Ramsey fringes formed by N query pulses with time delays ($n\frac{T}{N}$, $n = 1 \dots N$) between the CPT pulse and each query pulse. Peak intensity of the central fringe is enhanced due to constructive interference at the fringe center $\Delta = 0$ for N Ramsey fringes. Other aspects of interference such as fringe width, secondary fringes, and

fringe spacing can be inferred from a mathematical model described later in Eq. (2) using Fourier analysis of the pulse sequence. The frequency stability of the Ramsey clock is inversely proportional to the SNR of the central fringe.¹ The signal associated with the peak amplitude of the central fringe can be defined as $S = \eta C P_{out}$ where η is the detector sensitivity, in units of Volt/Watt, and P_{out} is the peak output power corresponding to the central fringe. In Figs. 4(a)–4(c), the peak amplitude of the central fringe is found to increase with N . In fact, comparing the results in Fig. 4(c) for $N = 10$ with Fig. 3(b) for $N = 1$ (SQT), one finds that the peak amplitude of the central fringe has been increased by approximately 1.7 times. Thus, RQT produces a single-peaked Ramsey fringe with higher signal, S and higher contrast, C than SQT. The contrasts in our experiments were measured to be approximately 59%, 74%, 76%, and 73% for $N = 1, 3, 5,$ and 10 query pulses, respectively. The enhancement in C for $N = 10$ was found to be approximately 1.24 which is smaller than the enhancement in S due to an increase in the fringe background.

Assuming that the noise in the signal originates only from the photon shot-noise of P_{out} , the SNR for an averaging time of one second can be expressed as $C\sqrt{\frac{P_{out}}{h\nu}} = C\sqrt{N_p}$ (\sqrt{Hz}), where N_p is the number of photons detected per second. Thus, a high SNR can also be expected due to high contrast C of the central fringe produced by RQT. This in turn can result in increased frequency stability of the clock. This aspect is discussed in more detail later by taking into account the pulsed operation regime of the Ramsey clock.

We simulated Ramsey fringes using the three-level model and measured the contrasts and peak amplitudes of the central fringes produced by RQT for different values of N . Figures 5(a)–5(c) show the simulated Ramsey spectra using RQT with $N = 3, 5,$ and 10 , respectively. The simulation parameters were chosen to be the same as those for the SQT simulations, except that the time-intervals between query pulses were chosen as $T_1 = T_2 \dots = T/N$ and $T = 1.5 \text{ ms}$. These spectra show striking similarity with the experimental results shown in Figs. 4(a)–4(c). Constructive interference of

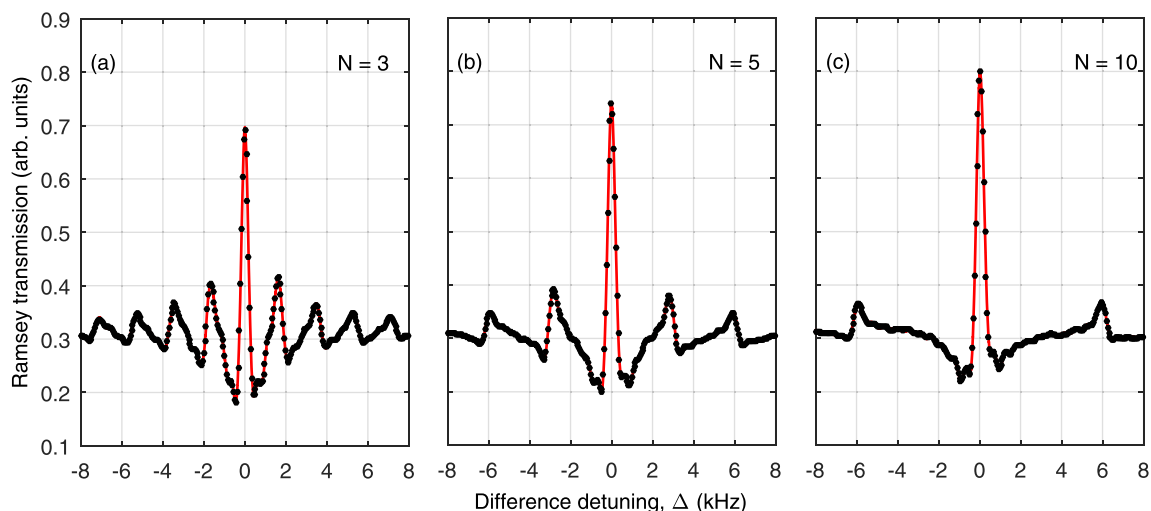


FIG. 4. Experimentally acquired Ramsey spectra via RQT using (a) $N = 3$ (b) $N = 5$, and (c) $N = 10$ query pulses in the pulse cycle. The average optical power used in the CPT pulse is approximately $24 \mu\text{W}$.

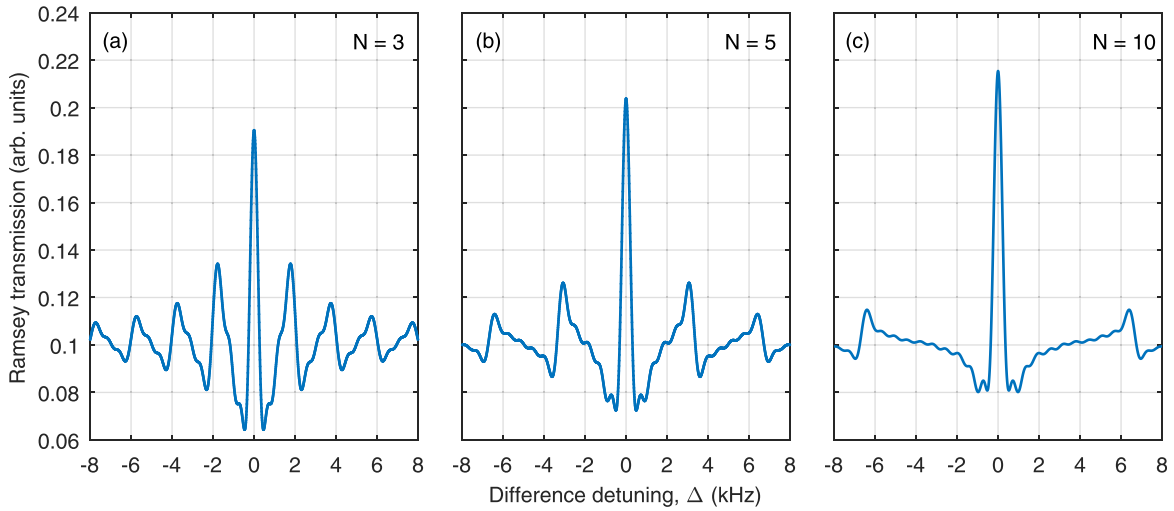


FIG. 5. Simulated Ramsey spectra obtained using (a) $N = 3$ (b) $N = 5$, and (c) $N = 10$ query pulses in the RQT pulse cycle. The parameters used in simulations are $\tau_c = 500 \mu\text{s}$, $T = 1.5 \text{ ms}$, $\tau_q = 1 \mu\text{s}$, $\Omega = \Gamma/100$, $\Gamma = 6 \text{ MHz}$, $\delta = 0$, and $\gamma = 200 \text{ Hz}$.

all Ramsey fringes at the fringe center $\Delta = 0$ creates a single-peaked Ramsey fringe with high contrast. By adding more query pulses to the pulse cycle, the side fringes are found to be adequately suppressed and separated with respect to the central fringe. We also observed in Figs. 4(a)–4(c) and 5(a)–5(c) a broadening of the central fringe-width, $\Delta\nu$ from $1/2T = 333 \text{ Hz}$ as N is increased. For large N , the fringe-width nearly doubles in comparison to the fringe-width observed at $N = 1$. We explain this later using a simple model based on the Fourier analysis of the pulse sequence. Figures 6(a) and 6(b) show variations in contrast and peak amplitude of the central fringe with N , obtained from our experiments and simulations. Both show a similar trend and consistency, i.e., the contrast and the peak amplitude grow quickly for a small value

of N between 2 to 5 and reach a steady-value (or decline) for large N exceeding $N = 15$. The lack of quantitative agreement between the experimental results and the simulation results is attributed to the facts that the experimental measurements include the effect of signal averaging and integration involved in the boxcar, and the theoretical model is incomplete due to reasons discussed earlier.

Next, we provide a simple understanding of the Ramsey spectrum produced by RQT using Fourier analysis of the pulse sequence.⁴¹ To simplify our analysis, we assume a periodic train of square pulses of duration τ_q , time-interval T/N , and exponentially decaying pulse amplitudes $e^{-n\gamma\frac{T}{N}}$, where $n = 1 \dots N$. Under this approximation, the Ramsey spectrum can be expressed analytically as

$$R(\Delta) = \text{sinc}\left(\frac{\Delta\tau_q}{2\pi}\right) \otimes \frac{e^{-\gamma T} \left\{ \cos\left[(N+1)\frac{\Delta \cdot T}{N}\right] - e^{-\gamma\frac{T}{N}} \cos(\Delta \cdot T) \right\} - \cos\left(\frac{\Delta \cdot T}{N}\right) + e^{-\gamma\frac{T}{N}}}{2 \left[\cos\left(\frac{\Delta \cdot T}{N}\right) - \cosh\left(\gamma\frac{T}{N}\right) \right]}, \quad (2)$$

where \otimes represents convolution, the first-term represents the fringe envelope corresponding to FT of the query pulse, and the second-term represents Ramsey fringes produced by the periodic pulse train. Considering no decay ($\gamma = 0$), the second expression reduces to a familiar mathematical function $\frac{\sin\left[\frac{(2N+1)\Delta \cdot T/2N}{2 \sin[\Delta \cdot T/2N]}\right]}$ which can be analyzed to study the characteristics of Ramsey fringes formed due to RQT. For $N = 1$, the function reduces to $\cos(\Delta \cdot T)$ which corresponds to traditional Ramsey fringes produced by SQT. The separation between the peaks of adjacent Ramsey fringes is found to be $\Delta_{p-p} = N/T \simeq N$ (666 Hz) which matches very well with our results shown in Figs. 4(a)–4(c) and 5(a)–5(c). We also estimated the null-to-null width of the central Ramsey fringe which is given by $\Delta_{n-n} = [2N/(2N+1)](1/T)$. This

suggests that Δ_{n-n} increases with N leading to broadening of the central fringe as previously observed in Figs. 4(a)–4(c) and 5(a)–5(c). Compared to the null-to-null fringe-width at $N = 1$, the fringe-width for $N = 10$ is increased by approximately 44%. The Fourier analysis also predicts that the peak amplitude of the central Ramsey fringe at $\Delta = 0$ will become N times larger, thereby increasing the contrast N fold. In the presence of pulse amplitude decay ($\gamma \neq 0$), the enhancement factor can be found from Eq. (2) to be $\frac{e^{\gamma T} - 1}{e^{\gamma T/N} - 1}$. However, this model is somewhat simplistic and does not provide a proper prediction of contrast enhancement. As such, the primary purpose of this model is to provide a qualitative understanding of the origin and characteristics of Ramsey fringes formed by RQT.

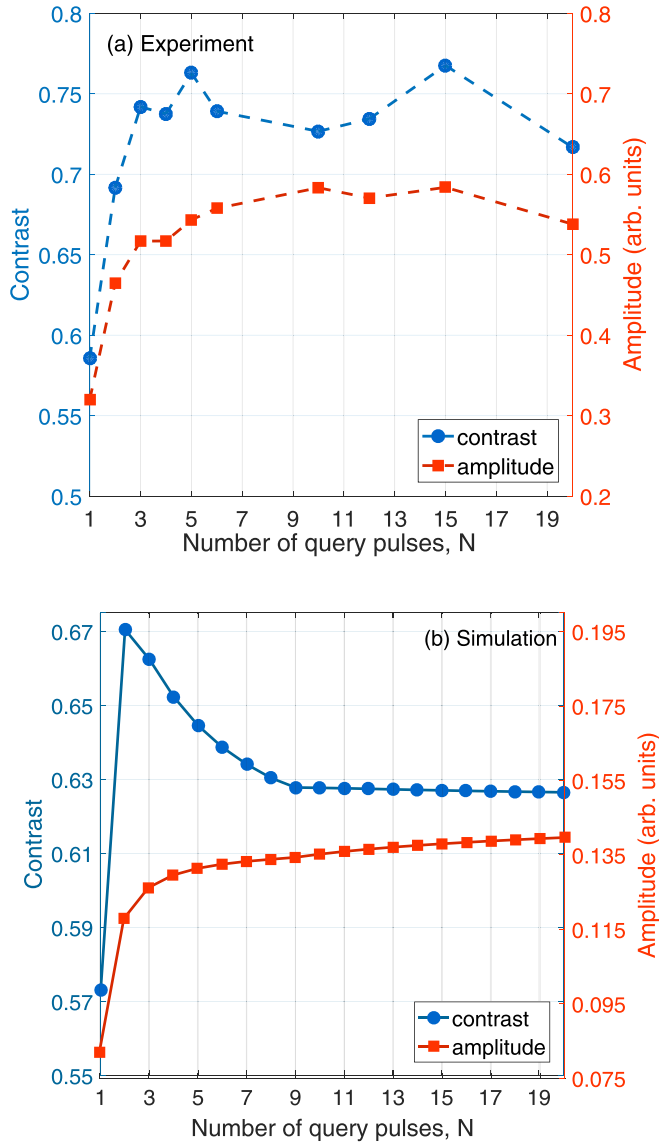


FIG. 6. Variation in the central fringe contrast and amplitude with N number of query pulses used in our (a) experiment, and (b) simulation.

We measured the frequency stability performance of the prototype Ramsey clock by employing SQT and RQT. During clock operation, the output frequency of the TSVCO was locked to the peak of the central Ramsey fringe by engaging the clock servo. The frequency stability (or ADEV, σ_y) of the locked TSVCO was measured with an ADEV measurement test-probe by referencing it to a rubidium frequency standard. Figure 7 shows ADEV, $\sigma_y(\tau)$ as a function of the averaging (or integration) time, τ for $N = 1$ and $N = 10$ query pulses. The fundamental photon shot-noise limited frequency stability^{1,42} of the Ramsey clock is given by the following expression:

$$\sigma_y(\tau) = \frac{1}{Q \cdot SNR} \sqrt{\frac{\tau_p}{(N \tau_q)}} \tau^{-\frac{1}{2}}, \quad (3)$$

where $Q = \omega_{hf}/\Delta\omega$ represents the quality factor of the central Ramsey fringe and $\Delta\omega$ corresponds to the central fringe-width. Due to pulsed operation of the Ramsey clock, σ_y in

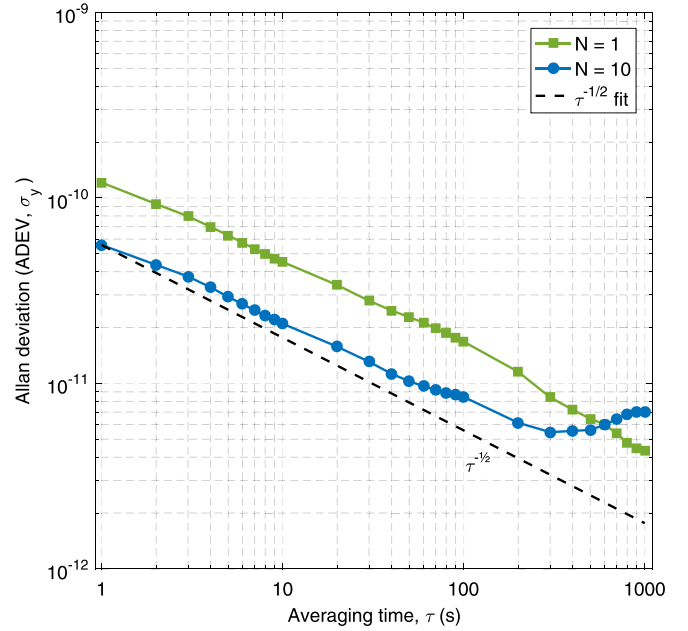


FIG. 7. Frequency stability (or ADEV) performance of the rubidium Ramsey clock measured with SQT (green squares) and RQT with $N = 10$ (blue circles). The dashed line represents a fit to $\sigma_y(\tau) = 5.58 \times 10^{-11} \tau^{-1/2}$.

Eq. (3) includes an additional square-root factor as the ratio of the cycle period $\tau_p (= 2.1 \text{ ms})$ to the total detection time window, $(N\tau_q)$. For the CPT clock which uses a continuous-mode detection, this factor is one. In the case of RQT, using multiple query pulses gives an advantage of improving $\sigma_y(\tau)$ by $1/\sqrt{N}$ simply because of the extended detection time window. This is in addition to the SNR improvement that we have discussed previously in the context of RQT. Using $SNR = C\sqrt{N_p}$ and Q (obtained from the experiment) in Eq. (3), we have estimated the shot-noise limited $\sigma_y^{sn}(\tau) \approx 1 \times 10^{-11}$ ($\tau = 1 \text{ s}$) for RQT, which corresponds to an improvement by a factor 2.7 compared to $\sigma_y^{sn}(\tau)$ for SQT. Broadening of the fringe-width and corresponding reduction in Q have been included while estimating $\sigma_y^{sn}(\tau)$ for RQT. It should be noted that in clock experiments, various classical noise sources such as laser intensity noise, laser frequency noise, phase noise of the oscillator, and electronic detection noise often dominate, and tend to stay well above the photon shot-noise level in the low-frequency limit. We measured the experimental frequency stability from Fig. 7 in the presence of such sources of noise, and observed that RQT with $N = 10$ exhibited better initial short-term stability $\sigma_y^{\text{exp}}(\tau) \simeq 5.6 \times 10^{-11}$ ($\tau = 1 \text{ s}$), which corresponds to an improvement nearly by a factor 2.2 compared to SQT with the $N = 1$ case. As seen in Fig. 7, improved $\sigma_y(\tau)$ with RQT was observed for τ ranging up to nearly 100s and $\sigma_y \simeq 8.4 \times 10^{-12}$ was reached at $\tau = 100 \text{ s}$, closely matching $\tau^{-1/2}$ fit generated from a starting stability of 5.6×10^{-11} ($\tau = 1 \text{ s}$) in Fig. 7. For τ exceeding 300s, the long-term stability with RQT started degrading in comparison to SQT. Our experimental system has several sources of noise and drifts, arising from active cell temperature control, EOM instability, magnetic field variation in the cell environment, etc. Some of these sources are affecting the long-term performance of

RQT differently from SQT. We are currently modifying our experimental design in order to minimize these sources of noise so that in future we will be able to improve the long-term performance of the Ramsey clock with RQT.

IV. CONCLUSIONS

We have demonstrated RQT as a new interrogation method in pulsed CPT for generating a single-peaked, high contrast Ramsey fringe. Our study shows significant improvement in contrast of the central Ramsey fringe along with reduction in the amplitude of the side fringes. We have developed theoretical models to calculate and analyze Ramsey spectra generated by different numbers of query pulses used in the pulse cycle, and shown close agreements between our theory and experimental results. We have also employed RQT in a rubidium Ramsey clock experiment and showed that the stability of the clock is improved in comparison to the conventional single query approach for averaging time up to nearly 100 s. Our results suggest that RQT can be used as a competitive technique in pulsed CPT for improving the performance of a compact Ramsey clock.

ACKNOWLEDGMENTS

The authors acknowledge the support received from the NASA-MIRO (NNX15AP84A), NASA-EPSCoR (80NSSC17M0026), NSF-CREST (1242067), and DoD HBCU/MI (62818-PH-REP) grants for conducting this research.

- ¹J. Vanier, "Atomic clocks based on coherent population trapping: A review," *Appl. Phys. B* **81**, 421–442 (2005).
- ²S. Knappe, "MEMS atomic clocks," in *Comprehensive Microsystems*, edited by Y. Gianchandani, O. Tabata, and H. Zappe (Elsevier, 2007), Vol. 3, pp. 571–612.
- ³V. Shah and J. Kitching, "Advances in coherent population trapping for atomic clocks," *Adv. At., Mol. Opt. Phys.* **59**, 21–74 (2010).
- ⁴E. E. Mikhailov, T. Horrom, N. Belcher, and I. Novikova, "Performance of a prototype atomic clock based on lin|lin coherent population trapping resonances in Rb atomic vapor," *J. Opt. Soc. Am. B* **27**, 417 (2010).
- ⁵D. Budker *et al.*, "Resonant nonlinear magneto-optical effects in atoms," *Rev. Mod. Phys.* **74**, 1153 (2002).
- ⁶S. N. Nikolić, M. Radonjić, N. M. Lučić, A. J. Krmpot, and B. M. Jelenković, "Transient development of Zeeman electromagnetically induced transparency during propagation of Raman-Ramsey pulses through Rb buffer gas cell," *J. Phys. B: At. Mol. Opt. Phys.* **48**, 045501 (2015).
- ⁷G. Alzetta, A. Gozzini, L. Moi, and G. Orriols, "An experimental method for the observation of r.f. transitions and laser beat resonances in oriented Na vapour," *Nuovo Cimento B* **36**, 5 (1976).
- ⁸E. Arimondo, "Coherent population trapping in laser spectroscopy," in *Progress in Optics XXXV*, edited by E. Wolf (Elsevier Science, 1996), p. 257.
- ⁹R. Wynands and A. Nagel, "Precision spectroscopy with coherent dark states," *Appl. Phys. B: Lasers Opt.* **68**, 1–25 (1999).
- ¹⁰M. Merimaa, T. Lindvall, I. Tittonen, and E. Ikonen, "All-optical atomic clock based on coherent population trapping in 85Rb," *J. Opt. Soc. Am. B* **20**, 273 (2003).
- ¹¹M. S. Shahriar, P. R. Hemmer, D. P. Katz, A. Lee, and M. G. Prentiss, "Dark-state-based three-element vector model for the stimulated Raman interaction," *Phys. Rev. A* **55**, 2272–2282 (1997).
- ¹²J. Vanier, M. W. Levine, D. Janssen, and M. Delaney, "Contrast and line-width of the coherent population trapping transmission hyperfine resonance line in 87Rb: Effect of optical pumping," *Phys. Rev. A* **67**, 065801 (2003).
- ¹³T. Zanon *et al.*, "High contrast Ramsey fringes with coherent-population-trapping pulses in a double lambda atomic system," *Phys. Rev. Lett.* **94**, 193002 (2005).
- ¹⁴T. Zanon *et al.*, "Observation of Raman-Ramsey fringes with optical CPT pulses," *IEEE Trans. Instrum. Meas.* **54**, 776–779 (2005).
- ¹⁵S. Guérandel *et al.*, "Raman-Ramsey interaction for coherent population trapping Cs clock," *IEEE Trans. Instrum. Meas.* **56**, 383–387 (2007).
- ¹⁶G. S. Pati, K. Salit, R. Tripathi, and M. S. Shahriar, "Demonstration of Raman-Ramsey fringes using time delayed optical pulses in rubidium vapor," *Opt. Commun.* **281**, 4676–4680 (2008).
- ¹⁷R. Boudot, S. Guérandel, E. de Clercq, N. Dimarcq, and A. Clairon, "Current status of a pulsed CPT Cs cell clock," *IEEE Trans. Instrum. Meas.* **58**, 1217–1222 (2009).
- ¹⁸G. S. Pati, F. K. Fatemi, and M. S. Shahriar, "Observation of query pulse length dependent Ramsey interference in rubidium vapor using pulsed Raman excitation," *Opt. Express* **19**, 22388–22401 (2011).
- ¹⁹Y. Yano and S. Goka, "Pulse excitation method of coherent-population-trapping suitable for chip-scale atomic clock," *Jpn. J. Appl. Phys., Part 1* **51**, 122401 (2012).
- ²⁰F. X. Esnault *et al.*, "Cold-atom double- Λ coherent population trapping clock," *Phys. Rev. A - At. Mol. Opt. Phys.* **88**, 042120 (2013).
- ²¹I. Yoshida *et al.*, "Line-shape comparison of electromagnetically induced transparency and Raman Ramsey fringes in sodium vapor," *Phys. Rev. A - At. Mol. Opt. Phys.* **87**, 023836 (2013).
- ²²P. Yun, J. M. Danet, D. Holleville, E. De Clercq, and S. Guérandel, "Constructive polarization modulation for coherent population trapping clock," *Appl. Phys. Lett.* **105**, 231106 (2014).
- ²³P. R. Hemmer, M. S. Shahriar, V. D. Natoli, and S. Ezekiel, "Ac Stark shifts in a two-zone Raman interaction," *J. Opt. Soc. Am. B* **6**, 1519 (1989).
- ²⁴G. S. Pati, Z. Warren, N. Yu, and M. S. Shahriar, "Computational studies of light shift in a Raman-Ramsey interference-based atomic clock," *J. Opt. Soc. Am. B* **32**, 388–394 (2015).
- ²⁵Y. Yano, W. Gao, S. Goka, and M. Kajita, "Theoretical and experimental investigation of the light shift in Ramsey coherent population trapping," *Phys. Rev. A - At. Mol. Opt. Phys.* **90**, 013826 (2014).
- ²⁶M. A. Hafiz *et al.*, "A high-performance Raman-Ramsey Cs vapor cell atomic clock," *J. Appl. Phys.* **121**, 104903 (2017).
- ²⁷E. Blanshan, S. M. Rochester, E. A. Donley, and J. Kitching, "Light shifts in a pulsed cold-atom coherent-population-trapping clock," *Phys. Rev. A* **91**, 041401 (2015).
- ²⁸A. Horsley *et al.*, "Imaging of relaxation times and microwave field strength in a microfabricated vapor cell," *Phys. Rev. A - At. Mol. Opt. Phys.* **88**, 063407 (2013).
- ²⁹T. Scholtes, S. Woetzel, R. IJsselsteijn, V. Schultze, and H. G. Meyer, "Intrinsic relaxation rates of polarized Cs vapor in miniaturized cells," *Appl. Phys. B: Lasers Opt.* **117**, 211–218 (2014).
- ³⁰M. Gharavipour *et al.*, "Optically-detected spin-echo method for relaxation times measurements in a Rb atomic vapor," *New J. Phys.* **19**, 063027 (2017).
- ³¹P. Yun *et al.*, "Multipulse Ramsey-CPT interference fringes for the 87 Rb clock transition," *Europhys. Lett.* **97**, 63004 (2012).
- ³²Y. Y. Jau, E. Miron, A. B. Post, N. N. Kuzma, and W. Happer, "Push-pull optical pumping of pure superposition states," *Phys. Rev. Lett.* **93**, 160802 (2004).
- ³³X. Liu, J. Mérolla, and S. Guérandel, "Ramsey spectroscopy of high-contrast CPT resonances with push-pull optical pumping in Cs vapor," *Opt. Express* **21**, 12451–12459 (2013).
- ³⁴X. L. Sun *et al.*, "Investigation of Ramsey spectroscopy in a lin-par-lin Ramsey coherent population trapping clock with dispersion detection," *Opt. Express* **24**, 4532 (2016).
- ³⁵S. Zibrov, V. L. Velichansky, A. S. Zibrov, A. V. Taichenachev, and V. I. Yudin, "Experimental investigation of the dark pseudoresonance on the D1 line of the 87Rb atom excited by a linearly polarized field," *J. Exp. Theor. Phys. Lett.* **82**, 477 (2005).
- ³⁶Z. Warren, S. M. Shahriar, R. Tripathi, and G. S. Pati, "Experimental and theoretical comparison of different optical excitation schemes for a compact coherent population trapping Rb vapor clock," *Metrologia* **54**, 418 (2017).
- ³⁷J. Snoddy, Y. Li, F. Ravet, and X. Bao, "Stabilization of electro-optic modulator bias voltage drift using a lock-in amplifier and a proportional-

integral-derivative controller in a distributed Brillouin sensor system,” *Appl. Opt.* **46**, 1482 (2007).

³⁸S. Goka, “85 Rb Coherent-population-trapping atomic clock with low power consumption,” *Jpn. J. Appl. Phys., Part 1* **48**, 082202 (2009).

³⁹S. Goka, “85Rb D1-line coherent-population-trapping atomic clock for low-power operation,” *Jpn. J. Appl. Phys., Part 1* **49**, 062801 (2010).

⁴⁰M. S. Shahriar *et al.*, “Evolution of an N-level system via automated vectorization of the Liouville equations and application to optically controlled polarization rotation,” *J. Mod. Opt.* **61**, 351–367 (2014).

⁴¹C. J. Foot, *Atomic Physics* (Oxford University Press, USA, 2005).

⁴²J. Lin, J. Deng, Y. Ma, H. He, and Y. Wang, “Detection of ultrahigh resonance contrast in vapor-cell atomic clocks,” *Opt. Lett.* **37**, 5036 (2012).